

Logging-while-drilling and wireline velocities: Site NGHP-01-10, Krishna-Godavari Basin, India

P. Jaiswal^{1*}, S. Al-Bulushi¹ and P. Dewangan²

* Email: priyank.jaiswal@okstate.edu, Phone: 405 744 6041, Fax: 405 334 7841

1. Boone Pickens School of Geology, Oklahoma State University, Stillwater, Oklahoma 74078, USA
2. CSIR-National Institute of Oceanography, Dona Paula, Goa, 403004, India

Abstract:

At site NGHP-01-10, Krishna-Godavari Basin, India, the Wireline tool recorded higher porosity and sonic velocities in hydrate-bearing sediments compared to the Logging-While-Drilling (LWD) tool in close proximity (~10 m). Using a novel rock physics model that implements random fractures in unconsolidated sediments using Hashin-Shtrikman bounds, we show that difference in physical properties could be due to intra-site difference in pattern of hydrate-filled fractures rather than difference in the volume of hydrate. Our fracture-inclusive model suggests that between the two holes the porosity and hydrate saturation of the background sediments is similar while porosity and hydrate saturation of fractures considerably change, in turn changing the overall sonic log character. Relative changes in hydrate saturation between sediments and fractures at 90 meters below the sea floor (mbsf) depth (a prominent seismic horizon), suggests that fracture-filling hydrate could have partly originated in the background sediments and migrated due to fluid flow. The volume fracture profile of hydrate (fracture porosity * fracture saturation) between the two holes further suggests that excess fractures in the Wireline hole may not be in-situ but rather a manifestation of the drilling compounded with time lapse in data recording. Frequently reported, worldwide, intra-site variability in hydrate saturation from LWD and Wireline logs in close proximity could be more methodological than geological.

Keywords: Gas hydrate; Fracture; Rock-Physics

Introduction

Hydrate is an ice-like structure made up of gas (mostly methane) and water stable under a narrow range of pressure (P) and temperature (T). In marine conditions, it exists within top few hundred meters of the seafloor. In theory, hydrate can form wherever light hydrocarbon gases saturate pore waters between the seafloor and the base of gas hydrate stability. Hydrate precipitates from the pore water when the concentration of the dissolved gas exceeds its solubility. Hydrate forms condensed gas reservoirs; 1 m³ of hydrate contains ~164 m³ gas at surface P and T (Sloan and Koh, 2007). Pressure – temperature conditions along continental margins favor presence of enormous quantities of hydrate (Milkov, 2004). Due to its widespread occurrence, large volumetric and restricted stability, hydrate can play significant role in climate change (Gu et al., 2011), seafloor stability (Brown et al., 2006), and energy security (Boswell and Collett, 2011).

The most popular way of hydrate resource assessment is through drilling and logging. Logging is like a surface geophysical survey done in a borehole, only with very limited survey aperture due to close source and receiver spacing. There are two methods of logging. The Wireline method has been in practice since early 19th century. In this method an assembly of tools are sent into a borehole after the borehole has been completely drilled, the tools acquire and store the data; the time-lapse between drilling and data recording can be several tens of hours. These data can only be downloaded after the tools have been retrieved. The logging-while-drilling (LWD) method was introduced to overcome this limitation so that decisions on well trajectory could be made based on *in-situ* information in real time. In general, in a LWD assembly, three accelerometers (for inclination) and three magnetometers (for azimuth) are orthogonally mounted within the tool assembly. These directional sensors along with other sensors (density, porosity, acoustic, etc.) are connected to a “pulsar” unit which converts and sends the sensor data to surface using "mud pulse telemetry," i.e., by varying the drilling fluid (mud) pressure. The pressure fluctuations are decoded on surface for data. After the LWD tools are retrieved, a comprehensive dataset can be prepared. Although the time-lapse in the Wireline method could lead to the hole degradation, the biggest advantage of Wireline is a possibility of core retrieval.

Hydrate resource assessment along the Indian continental margins was done in 2007 through a joint venture between United States Geological Survey and Directorate General of Hydrocarbons, India. In the expedition, known as NGHP-01, both coring and LWD and Wireline logging operations were performed. One of the most comprehensive datasets in the entire NGHP-01 expedition were acquired at

site NGHP-01-10 (hereafter Site 10) in the Krishna-Godavari (KG) Basin where four holes, 10A – D, were drilled within 20 m for coring and logging (Collett et al., 2008). At Hole 10B, dedicated to coring, 128m of hydrate-filled fractured sediments were recovered. The cores were depressurized at three depth locations. Hydrate saturation in lower 20% range was inferred at all three locations. Hole 10A (10m NW of 10B) was logged using LWD method and is hereafter referred to as the LWD hole. Hole 10D (10m NW of 10A) was logged using Wireline and is hereafter referred to as the Wireline hole. What surprised the hydrate community was very differently looking LWD and Wireline signatures despite the holes being in such close proximity.

Although depressurizing core samples provide most accurate hydrate quantities, cost considerations often dictate quantification to be performed indirectly from well logs. At Site 10, the quest has been to understand the reason(s) behind differences in Wireline and LWD logs and relate them to hydrate saturation inferred from depressurization tests. In their pioneering work on Site 10, Lee and Collett (2009) suggested that dissociation of hydrate into free gas during the LWD drilling could be responsible for overall lower sonic velocities at 10A. It can be argued that higher porosity (and higher V_p) at the Wireline hole compared to LWD hole at Site 10 is a coincidence and as a result of the intrasite variability in hydrate-bearing sediment conditions. However, higher-than-LWD Wireline V_p is also observed in the Cascadia (Goldberg et al., 2008) and the Ulleang basin (Kim et al., 2011), suggesting that this phenomenon might be a consequence of the drilling technology.

Till date, saturation and state (grain displacing, pore filling, etc.) of hydrate at Site 10 has not been agreed upon unequivocally. For example, using Archie equation (which assumes isotropic clean sandstones) on Wireline resistivity log, Collett et al. (2008) estimated ~85% saturation between 27 and 90 meters below the sea floor (mbsf) which was a marked increase over that derived from X-ray CT measurements by Rees et al. (2011) within the same interval. Lee and Collett's (2009) velocity modeling with three-phase Biot-type equation reduced the estimated hydrate saturation to ~65%, which is still substantially higher than core depressurization tests.

The core from hole 10B clearly shows fractures, which have been incorporated in the rock models in numerous ways but with implicit anisotropic implications in all cases. These models have however yielded limited success. Lee and Collett (2009) attempted to match P- and S- wave velocities (V_p and V_s) with a common fracture dip. At $\sim 84^\circ$ dip, log and model V_p were most similar but V_s still had discrepancies, which they attributed to not knowing the alignment of S-wave sensor to the fractures.

Cook et al. (2010) modified Archie's type equation to account for veins at sub-vertical angles and showed that dipping fractures can also create electrical anisotropy; their model resistivity were most similar to log at 70–80° fracture dip but had high uncertainties. Similarly, Ghosh et al. (2010) modified a grain-displacing model to place hydrates in oblate ellipsoids to imitate the fractures. Their results were comparable to the real hydrate saturation but uncertainties saturation estimation were as much as 50% at various depths. The rock physics models used for hydrate quantification at Site 10 may need to be revisited.

Given differences in geophysical signatures, it is desirable to understand which method, Wireline or LWD, is more reliable for hydrate quantification. In this paper we show that both methods are equally good provided the rock models are able to account for the changes in sediment which results from drilling. It is intuitively expected that drilling in unconsolidated sediments will create fractures. As fractures have higher permeability than the background sediments, in presence of fluid flow they tend to accumulate more hydrates over time (Bhatnagar et al., 2007). In our case, this becomes relevant if it turns out that the time-lapse between drilling and data recording in the Wireline method is adequate for re-distribution of hydrate within the stability zone such that it has measureable effect on sonic velocities. We present preliminary evidences that at Site 10 this could indeed be the case. Although we are not refuting the possibility of previous models, a more thorough, both experimental and numerical, investigation using additional data from other sites is needed for confirmation.

Most of the models applied at Site 10 till date, whether anisotropic or not, are exclusive, i.e., hydrate are either present only in fractures or only in background. We hypothesize that at Site 10 hydrate is concurrently present in fracture as well as background sediments. The rational is to facilitate separation of hydrate-filled fractures from hydrate-filled background sediments at both LWD and Wireline holes. The impetus for our hypothesis comes from observation made by Collett et al. (2008) in the NGHP-10B-18Y core, "the bulk of the gas hydrate in this core must be in a more distributed form that is below the resolution of the X-ray images, or indeed the naked eye." Collett et al.(2008) further speculated that the dissipated hydrate could have displace pore water or sediment grain, in both cases potentially contributing to an increase in elastic velocities. We also posit that fracture-driven anisotropy at Site 10 also may not be as strong as previously imagined; equal-area lower-hemisphere projection of fractures in Hole 10A from Cook et al.(2010)and Hole 10B from Rees et al. (2011) suggest randomness in fracture orientation.

This paper is organized as follows. We first present a model where fractures can be incorporated in the rock using a mixing law that follows the Hashin-Shtrikman(HS) bounds (Wang, 2001). The biggest advantage of this model is its flexibility – it allows accounting for the density and connectivity of fractures and simultaneous placement of hydrate in sediments (as either pore-filling or grain displacing mode) and fractures. Further, the model automatically assumes random fractures with no bearing on system anisotropy. Next, using the model, we show that the hydrate saturation from depressurization test can be distributed within the background and fractures in the Wireline hole such that the V_P and V_S logs are closely replicated. Following this, we show that maintaining the same saturation and porosity of the background sediments at the LWD hole, a lower V_P can be explained by changing the fracture connectivity and fracture porosity. Finally, we discuss the global applicability of this model.

Method

Estimating elastic velocities in porous rocks involves reconstructing elastic moduli of dry matrix and pore fluid separately followed by their union through Gassman's method (Chand et al., 2004). Nur et al. (1991) showed that at high effective pressures clean sandstones have a distinct relation between the bulk porosity and effective moduli; the trend is linear, arithmetic mean between pure quartz (zero porosity) and sand assemblage at critical porosity. As the rock becomes multi-mineral, different mixture components deform differently in response to the same seismic stress and the relation between the bulk porosity and the effective moduli becomes non-linear. For mixing grains in a Hashin-type assemblage (Hashin and Shtrikman, 1963) a pore topology that undergoes uniform deformation, two end-member trajectories in the modulus-porosity plane connecting zero and critical porosity have been proposed. Assemblage resembling soft core encased in a stiff shell follows the modified upper HS bounds (Gal et al., 1998) and that resembling stiff core encased by soft shell follow the modified lower HS bounds (Dvorkin and Nur, 1996).

We extend this line of thought to mix hydrate-filled fractures with sediments. The model assumptions are as follows. First, the rock is a combination of background sediments and hydrate-filled fractures. The "background sediments" refer to an assemblage of random spheres with fully interconnected pores (Helgerud et al., 1999). Second, hydrate-filled fractures are stiffer than the background sediments, which holds even in presence of fluids in the fractures. Its physical realization can be understood as follow. When fractures are created by hydrate, the hydrate tends to be at the interface

between fluid and sediments (Jain and Juanes, 2009). Two scenarios can be conceived. First, the fluid can be encased within a hydrate shell (Behseresht et al., 2008; Stern et al., 2004). Second, the fluids and hydrate could be separate. In either case, under seismic stress, the volume change of the hydrate-filled part of the fracture will be limited by hydrate. Therefore the hydrate-filled part of the fractures can be considered as a stiffer component. When the hydrate-filled fractures are disconnected (Figure 1a), they act like a stiffer core and the scenario can be realized using the lower HS bound. Similarly, when hydrate-filled fractures are interconnected (Figure 1b), they could act like a stiffer shell and the scenario can be realized using the modified upper HS bound. The term connected and disconnected are not intended to be indicative of the physical appearance of the fractures, but rather the manner in which hydrate are present within the fractures.

Consider a mixture comprising disconnected/interconnected hydrate- and brine-filled fractures (annotated D/I) and sediment. The total porosity of the system (ϕ_t) will be the sum of porosity of the background sediments (ϕ_s) and porosity of the fractures (ϕ_f). If $f_1 - f_3$ are the volume fractions of the background sediments, hydrate-filled fractures and brine-filled fractures, the bulk ($K^{D/I}$) and Shear ($G^{D/I}$) moduli of this mixture can be expressed through the general form of Hashin-Shtrikman bounds (Mavko et al., 2009) as:

$$K^{D/I} = \left[\sum_{i=1}^3 \frac{f_i}{K_i + \frac{4}{3} G_{(min/max)}} \right]^{-1} - \frac{4}{3} G_{(min/max)}; \quad G^{D/I} = \left[\sum_{i=1}^3 \frac{f_i}{G_i + Z_{(min/max)}} \right]^{-1} - Z_{(min/max)} \quad (1)$$

$$Z_{(min,max)} = \frac{1}{6} G_{(min/max)} \left(\frac{9K_{(min/max)} + 8G_{(min/max)}}{K_{(min/max)} + 2G_{(min/max)}} \right);$$

In Equation (1), Subscripts *min* and *max* refer to the minimum and maximum modulus of the individual minerals or fluids that make up the mixture. For example, the mixture described above is made up of quartz, clay, hydrates and brine. In Equation 1, K_{min} and G_{min} will be 2.37 GPa and 0 GPa corresponding to brine and K_{max} and G_{max} will be 36 GPa and 45 GPa corresponding to quartz (Table 1). V_P and V_S for the mixture can be expressed as:

$$V_P^{D/I} = \sqrt{\frac{K^{D/I} + \frac{4}{3} G^{D/I}}{\rho_b}}; \quad V_S^{D/I} = \sqrt{\frac{G^{D/I}}{\rho_b}} \quad (2)$$

In Equation (2), ρ_b is the bulk density of the system which is expressed as:

$$\rho_b = (1 - \phi_f) \cdot \rho_s + \phi_f \cdot \rho_f \quad (3)$$

In Equation (3) ρ_f is the density of hydrate-filled part of the fracture and ρ_s is the bulk density of the background sediment which in turn are calculated as follows:

$$\begin{aligned} \rho_f &= S_{hf} \rho_h + (1 - S_{hf}) \rho_w \\ \rho_s &= (1 - \phi_s) \rho_m + \phi_s \rho_{pf} \end{aligned} \quad (4)$$

In Equation (4), S_{hf} is the hydrate saturation in fracture, ρ_h , ρ_w , ρ_m and ρ_{pf} are densities of hydrate, brine, dry matrix of the background sediment and pore fluid of the background sediments respectively. The pore fluid in Equation 4 could be replaced with brine if hydrate are not present in the background sediments. In case they are (say with saturation S_{hm}), depending on whether they have pore-filling or grain-displacing form, both ρ_m and ρ_{pf} can be modified accordingly (Dvorkin et al., 2003; Helgerud et al., 2000). When both hydrate and brine are present in fracture, the volume fractions of the mixture constituents in terms of ϕ_f can be expressed as, $f_1 = 1 - \phi_f$, $f_2 = \phi_f \cdot S_{hf}$, and $f_3 = \phi_f \cdot (1 - S_{hf})$. When hydrate and brine are separate in the fractures, for modeling stability it becomes necessary to merge the brine-filled part of the fracture with background sediment. We alter the porosity of the fracture and the background as $\phi_f^{new} = \phi_f - f_3$ and $\phi_s^{new} = \phi_s + f_3$. Due to the unconsolidated nature of the background sediments, their K and G are always computed using the modified lower HS bounds.

Application and results

Due to the physics of wave propagation, unknowns such as ϕ_s , ϕ_f , S_{hf} , S_{hs} , form of hydrate in the background sediments (pore-filling or load-bearing) and the nature of fracture connectivity (interconnected vs. disconnected) cannot be directly back-computed from elastic velocities. However, they can be made to serve as input to a rock physics model where the output is elastic velocities. Consequently, by changing the inputs and comparing the outputs the individual input parameters can be iteratively inferred. A robust rock physics should be able to take information about the rock fabric in a very detailed manner for computing the velocities. Such detail information is typically not available. There, for simplicity, certain assumptions are made. In our case we assume that a) ϕ_s is constant throughout the length of the borehole, and b) the form of hydrate in sediment does not

change from one borehole to another. The first assumption is based on the character of neutron porosity logs (Figure 2a) in both the LWD and Wireline hole, which suggests that the sediments are fairly uniform in nature. Due to a reasonable agreement with core porosity (Figure 2a) we use the neutron porosity as a proxy for ϕ_i in both holes.

We start our modeling at the Wireline hole with $\phi_s = 10\%$ (90% of total porosity is due to fractures) and $S_{hs} = 0$ (all hydrate are in fracture). Then, we compute V_P and V_S using equations 1 – 4 for the entire length of the Wireline log for both interconnected and disconnected cases; this constitutes a single forward modeling run. For every forward model, we compute the error between predicted and log velocities for both interconnected and disconnected cases in a root-mean-square (RMS) sense as:

$$E_{RMS} = \frac{1}{n} \sqrt{\sum_{i=1}^n \frac{(V_P^{Pi} - V_P^{Oi})^2}{\sigma_P} + \sum_{i=1}^n \frac{(V_S^{Pi} - V_S^{Oi})^2}{\sigma_S}} \quad (5)$$

In Equation (5), n is the number of log data points (460), superscripts Pi and Oi denote the i^{th} predicted and observed data point and σ_P and σ_S are standard deviations in the V_P and V_S logs respectively. Standard deviation implies variations with respect to a mean value. In the V_P and V_S logs, the mean could be thought of representing velocity of the background sediment, which is being considered rather homogenous in nature, while the standard deviation could be thought of perturbations physical property due to fractures. Considering individual logs as independent time series, the Wireline sonic log has a mean of 1.85 km/s and σ_P of 74 m/s, the Wireline shear-sonic log has a mean of 0.405 km/s and σ_S of 64 m/s and the LWD sonic log has a mean of 1.715 km/s and σ_P of 50 m/s.

Our model (Equation 1 – 4) is populated in a heuristic manner. The model inputs are porosity and saturation and the model output are the elastic velocities. The model has four input parameters - ϕ_f , ϕ_s , S_{hf} , and S_{hs} . The ϕ_f is computed as $\phi_t - \phi_s$, leaving only three independent parameters. In principle it is possible to vary the four input parameters such that V_P and V_S will be *independently* matched at every depth. However, this is not the goal. We aim to adjust the input parameters such that the LWD and Wireline elastic velocities are *simultaneously* matched (fitted at the level of their respective uncertainties). The only model constraint is the total saturation, S_{ht} , measured through core depressurization at three depth locations - 21% at 88 mbsf to 22% at 97 mbsf to 24% at 118 mbsf (Figure 2b). Thus, the ultimate goal of model building is not only to fit the elastic velocities but also to make sure that the input saturations are consistent with S_{ht} .

It is notable that despite large variation in elastic velocities (Figures 3), S_{ht} remains fairly consistent (standard deviation of 3%), which suggests that velocity variations could be due to factors other than variations in hydrate saturation. As previously observed, ϕ_t also has very little variation within the borehole encouraging us to keep the input parameters spatially invariant as much as possible. While building the model, we manually vary the input parameters in a trial and error manner such that $(\phi_r S_{hf} + \phi_s S_{hs}) / (\phi_r + \phi_s)$ remains within 3% of S_{ht} at their respective depth locations. Any change in our input parameters, mainly ϕ_s , physically implies that the lithology is changing. Therefore we change ϕ_s only when necessary.

We found that by dividing the stratigraphy into two units only, separating at 90 mbsf, we could not only fit the velocities to within their respective uncertainties but also honor S_{ht} ; within each depth interval the model parameters remain constant. In the expedition report although this depth is not reported as being clearly associated with change in sediment type, the LWD Resistivity-At-Bit (RAB) images are reported to lose strength below 90 mbsf (Collett et al., 2008). Additionally, in the seismic profile from Jaiswal et al. (2012b) a high amplitude horizon labeled H2 appears to be intersecting Site 10 wellbores at this depth. It is therefore possible that the sediment character, and consequently the mechanical strength, changes at this depth which has implications on fracture connectivity.

Within 65 – 90m depth, with $\phi_s = 55\%$ and $\phi_f = \phi_t - 55\%$ (Figure 2a), $S_{hs} = 15\%$ with hydrate in the load-bearing form and $S_{hf} = 30\%$, the Wireline V_P and V_S respectively falls within 74 m/s and 64 m/s of V_P and V_S simulated with interconnected fractures (Figures 3a and b). Within the same depth interval, the LWD V_P also falls within 50 m/s of the simulated V_P with interconnected fractures (Figure 3c) and same ϕ_s and S_{hs} as the Wireline hole but a higher S_{hf} (Figure 3d). Within 90 – 135 m depth, with $\phi_s = 55\%$ and $\phi_f = \phi_t - 55\%$ (Figure 2a), $S_{hs} = 23\%$ with hydrate in load-bearing form, and $S_{hf} = 22\%$, the Wireline V_P and V_S respectively falls within 74 m/s and 64 m/s of V_P and V_S simulated with interconnected fractures (Figures 3a and b). Within the same interval, the LWD V_P falls within 50 m/s of V_P simulated with fractures in interconnected mode (Figure 3c) with the same ϕ_s and S_{hs} as the Wireline hole, but a lower S_{hf} (Figure 3d).

The results can be summarized as follows: a) ϕ_s is spatially constant (55%), b) ϕ_f is higher in the Wireline hole (due to a higher ϕ_t); c) S_{hs} increases from 15% to 23% at 90 mbsf, the increase being same in both holes; d) S_{hf} decrease from 50% to 35% at 90msf in the LWD hole and from 30% to 22% in the Wireline hole; and e) the form of hydrate (grain displacing) remains same between the two holes.

Another interesting outcome is the hydrate volume fraction, which is the product of saturation and porosity (Figure 4); the background hydrate volume fraction remains the same in both the holes and is within <5% of each other in the fractures, which implies that the total volume of hydrate between the two holes are fairly similar. Thus, results strongly suggest that the elastic velocity variations between the two holes may not be due to changes in hydrate but rather due to changes in the local fracture abundance and connectivity and also in the manner hydrate occupy the fractures.

Discussion

Consistency of LWD and Wireline data has been a long standing debate (Brie et al., 1998; Goldberg et al., 2003; Market and Canady, 2006; Tang et al., 2007; Varsamis et al., 2000). Compared to the Wireline, in the LWD, the first receiver is closer to the source. As a result, while the Wireline can see up to 2-3 borehole diameter, LWD's depth of investigation is limited to within 1. Depending on the scale of drilling-induced-fractures (micro or larger), which in turn could depend on the rheology, LWD and Wireline can record different information. Briggs et al. (2004) has shown that in unconsolidated zone LWD shear velocity can be up to 10% lower than Wireline; compressional velocity however should remain near identical. Goldberg et al. (2008) additionally argue that in unconsolidated media LWD can have leaky modes. In our case, Figure 2a shows that the Wireline porosity is higher (by ~10%) than the LWD porosity. Collette et al. (2008) show that the analytically-estimated porosity of samples from the Wireline hole closely follow the LWD neutron porosity (Figure 2a), which provides a reason to suspect that the Wireline data may not be reflective of the in-situ conditions. It is hard for us to argue in favor of any particular method. We have shown that both methods can reveal same information when the rock-fabric is properly taken into account.

The value of 55% that we have obtained for ϕ_s is the same as what Daigle and Dugan (2010) obtain as "minimum possible porosity" in their flow rate calculation at Site-10 with the help of Athy's law. Their model assumes that all fractures at Site 10 are hydraulic in nature. However, observing the sub-horizontal hydrate-filled veins that require pore pressures to be equal to or greater than the vertical effective stress, they conclude that "it is therefore difficult to generate (all) the observed features by pore occlusion alone." We argue that even at the LWD hole it is possible that some fractures, most likely the sub-horizontals, could be a drilling related. In the LWD hole, the fracture connectivity changes at 90 mbsf from an interconnected mode above to a disconnected mode below. A change in connectivity could be responsible for the change in the observed LWD RAB image character. Fractures in the Wireline hole

appear to be interconnected throughout the length of the hole. If sediments in both holes were in the same state prior to drilling, then it is possible that the Wireline method could have changed the fracture connectivity.

Hydrate saturation in fractures in the LWD hole is more than the Wireline hole above 90m, and vice versa. If both holes evolved from the same initial sediment conditions, it is also possible that in the time-lapse between drilling and the data recording in the Wireline hole, the hydrate are redistributed within the newly formed fractures. In principle, the time-lapse in the Wireline drilling is adequate for the kinetics of hydrate decomposition and formation under appropriate P-T and fluid flow (Abay and Svartaas, 2011; Windmeier and Oellrich, 2013) but laboratory based experiments and testing this model with other data are necessary for confirmation. Connectivity of the fractures could also be related to resistivity. We compare the line scan images of two cores from the Wireline hole (10D) in Figure 5, 10D-12E from the high resistivity zone (77.8 mbsf) and 10D-22E from the low resistivity zone (145.1 mbsf). In the line scan images, the fractures appear as gray-to-white features in an otherwise dark background. Figure 5 suggests that a) both cores have high volume % of fractures, supporting our model which assumes 15 -20% ϕ_f (Figure 2a) and b) the core from the higher resistivity zone has a higher fracture connectivity.

Hydrate kinetics are fairly complicated and have multiple dependencies (Roosta et al., 2013; Vysniauskas and Bishnoi, 1983). The dynamic models of fluid encased in hydrate shell is not fully developed, stability of hydrate shell appears to be inverse proportional to the dissolved methane concentration (Chen et al., 2013). We think that the interconnected scenario could be associated with periods of rapid fracture growth where, due to a sudden increase in permeability and water flow, the saturation of the dissolved methane can be reduced. It is more likely that in this scenario the fluid will be encased in hydrate shell. The disconnected scenario could present more steady-state periods of fracture growth, where fluid and hydrate could be existing separately in the fractures.

Despite the obvious presence of fracture, we have demonstrated an isotropic rock model. However, we do not intend to imply that fractures do not create anisotropy, but rather that in this instance an isotropic model can also explain the data to a large extent. It is notable though that even at the seismic scale reasonable models have been obtained with isotropic approximation in the vicinity of Site 10 (Jaiswal et al., 2012a; Riedel et al., 2011). The rock model that we have presented can easily be extended into an anisotropic domain by following Bandyopadhyay (2009). Other variations, such as

using Gassmann's substitution to introduce the brine-filled part of the fracture into a mixture of hydrate-filled fracture and background sediments are also possible. Discrimination of these models however require that a reasonable estimate of fracture patterns and connectivity be made available *a-priori*, possibly though high-fidelity 3D imaging of high-resolution seismic data.

Conclusions:

Using a rock physics model that incorporates randomly oriented fractures in unconsolidated sediments using Hashin-Strickman bounds we have compared and contrasted elastic velocities and porosities from Wireline and LWD holes located 10m apart at site NGHP-01-10 in KG basin, India. Results suggest that both the LWD and the Wireline holes have comparable background porosity and hydrate saturation but different fracture porosity and connectivity. We conclude that higher V_P and porosity at the Wireline hole could be due to change in pattern of hydrate-filled fractures rather than a change in hydrate volume. We posit that the fracture patterns at the Wireline hole could have evolved from the LWD hole as a result of time-lapse between Wireline drilling and data acquisition. We contend that a similar argument may hold at other sites worldwide where intra-site variability in hydrate saturation has been reported between LWD and Wireline holes.

Acknowledgements:

Jack Dvorkin, Stanford University, was very vital in our understanding of rock physics. We also thank Ann Cook, Ohio State University, for her thoughts.

References:

Abay, H.K., Svartaas, T.M., 2011. On the kinetics of methane hydrate formation: a time-dependent kinetic rate model, Proceedings of the 7th International Conference on Gas Hydrates, Edinburgh, Scotland, United Kingdom.

Bandyopadhyay, K., 2009. Seismic Anisotropy: Geological Causes and Its Implications to Reservoir Geophysics, School of Earth Sciences. Stanford University, Stanford, p. 254.

Behseresht, J., Prodanovic, M., Bryant, S., Jain, A., Juanes, R., 2008. Mechanisms by which methane gas and methane hydrate coexist in ocean sediments, Offshore Technology Conference, Houston, Texas.

Bhatnagar, G., Chapman, W.G., Dickens, G.R., Dugan, B., Hirasaki, G.J., 2007. Generalization of gas hydrate distribution and saturation in marine sediments by scaling of thermodynamic and transport processes. American Journal of Science 307, 861-900.

Boswell, R., Collett, T.S., 2011. Current perspectives on gas hydrate resources. Energy & Environmental Science 4.

Brie, A., Endo, T., Hoyle, D., Codazzi, D., Esmersoy, C., Hsu, K., Denoo, S., Mueller, M.C., Plona, T., Shenoy, R., 1998. New directions in sonic logging. *Oilfield Review* 10, 40-55.

Briggs, V., Rao, R.V., Grandi, S.K., Burns, D.R., Chi, S., 2004. A comparison of LWD and wireline dipole sonic data. Massachusetts Institute of Technology. Earth Resources Laboratory.

Brown, H.E., Holbrook, W.S., Hornbach, M.J., Nealon, J., 2006. Slide structure and role of gas hydrate at the northern boundary of the Storegga Slide, offshore Norway. *Marine Geology* 229, 179-186.

Chand, S., Minshull, T.A., Gei, D., Carcione, J.M., 2004. Elastic velocity models for gas-hydrate-bearing sediments - a comparison. *Geophysical Journal International* 159, 573-590.

Chen, L., Sloan, E.D., Koh, C.A., Sum, A.K., 2013. Methane Hydrate Formation and Dissociation on Suspended Gas Bubbles in Water. *Journal of Chemical & Engineering Data*.

Collett, T., Riedel, M., Cochran, J., Boswell, R., Presley, J., Kumar, P., Sathe, A., Sethi, A., Lall, M.V., Sibai, V., 2008. Expedition 01 Initial Reports, New Delhi, India.

Cook, A.E., Anderson, B.I., Malinverno, A., Mrozewski, S., Goldberg, D.S., 2010. Electrical anisotropy due to gas hydrate-filled fractures. *Geophysics* 75, F173-F185.

Daigle, H., Dugan, B., 2010. Origin and evolution of fracture-hosted methane hydrate deposits. *Journal of Geophysical Research-Solid Earth* 115.

Dvorkin, J., Nur, A., 1996. Elasticity of high-porosity sandstones: Theory for two North Sea data sets. *Geophysics* 61, 1363-1370.

Dvorkin, J., Nur, A., Uden, R., Taner, T., 2003. Rock physics of a gas hydrate reservoir. *The Leading Edge* 22, 842-847.

Gal, D., Dvorkin, J., Nur, A., 1998. A physical model for porosity reduction in sandstones. *GEOPHYSICS* 63, 454-459.

Ghosh, R., Sain, K., Ojha, M., 2010. Effective medium modeling of gas hydrate-filled fractures using the sonic log in the Krishna-Godavari basin, offshore eastern India. *Journal of Geophysical Research-Solid Earth* 115.

Goldberg, D., Cheng, A., Blanch, J., Byun, J.M., Gullick, S., 2003. Analysis of LWD sonic data in low-velocity formations, 2003 SEG Annual Meeting. Society of Exploration Geophysicists.

Goldberg, D., Guerin, G., Malinverno, A., Cook, A., 2008. Velocity analysis of LWD and Wireline sonic data in hydrate-bearing sediments on the Cascadia Margin, Proceedings of the 6th International Conference on Gas Hydrates, Vancouver, Canada.

Gu, G., Dickens, G.R., Bhatnagar, G., Colwell, F.S., Hirasaki, G.J., Chapman, W.G., 2011. Abundant Early Palaeogene marine gas hydrates despite warm deep-ocean temperatures. *Nature Geosci* 4, 848-851.

- Hashin, Z., Shtrikman, S., 1963. A variational approach to the theory of the elastic behaviour of multiphase materials. *Journal of the Mechanics and Physics of Solids* 11, 127-140.
- Helgerud, M.B., Dvorkin, J., Nur, A., 2000. Rock physics characterization for gas hydrate reservoirs - Elastic properties, in: Holder, G.D., Bishnoi, P.R. (Eds.), *Gas Hydrates: Challenges for the Future*, pp. 116-125.
- Helgerud, M.B., Dvorkin, J., Nur, A., Sakai, A., Collett, T., 1999. Elastic-wave velocity in marine sediments with gas hydrates: Effective medium modeling. *Geophysical Research Letters* 26, 2021-2024.
- Jain, A.K., Juanes, R., 2009. Preferential Mode of gas invasion in sediments: Grain-scale mechanistic model of coupled multiphase fluid flow and sediment mechanics. *Journal of Geophysical Research-Solid Earth* 114.
- Jaiswal, P., Dewangan, P., Ramprasad, T., Zelt, C.A., 2012a. Seismic characterization of hydrates in faulted, fine-grained sediments of Krishna-Godavari Basin: Full waveform inversion. *Journal of Geophysical Research: Solid Earth* 117, B10305.
- Jaiswal, P., Dewangan, P., Ramprasad, T., Zelt, C.A., 2012b. Seismic characterization of hydrates in faulted, fine-grained sediments of Krishna-Godavari basin: Unified imaging. *J. Geophys. Res.* 117, B04306.
- Kim, G.Y., Yi, B.Y., Yoo, D.G., Ryu, B.J., Riedel, M., 2011. Evidence of gas hydrate from downhole logging data in the Ulleung Basin, East Sea. *Marine and Petroleum Geology* 28, 1979-1985.
- Lee, M.W., Collett, T.S., 2009. Gas hydrate saturations estimated from fractured reservoir at Site NGHP-01-10, Krishna-Godavari Basin, India. *J. Geophys. Res.* 114, B07102.
- Market, J., Canady, W.J., 2006. Dispersion corrections are not just for LWD dipole sonic tools, SPE Annual Technical Conference and Exhibition. Society of Petroleum Engineers, San Antonio, TX, USA
- Mavko, G., Mukerji, T., Dvorkin, J., 2009. *The Rock Physics Handbook*, Second ed. Cambridge University Press, Cambridge, England.
- Milkov, A.V., 2004. Global estimates of hydrate-bound gas in marine sediments: how much is really out there? *Earth-Science Reviews* 66, 183-197.
- Nur, A., Marion, D., Yin, H., 1991. Wave velocities in sediments, in: Hovem, J.M., Richardson, M.D., Stoll, R.D. (Eds.), *Shear waves in marine sediments*. Kluwer Academic Publishers.
- Rees, E.V.L., Priest, J.A., Clayton, C.R.I., 2011. The structure of methane gas hydrate bearing sediments from the Krishna-Godavari Basin as seen from Micro-CT scanning. *Marine and Petroleum Geology* 28, 1283-1293.
- Riedel, M., Collett, T.S., Shankar, U., 2011. Documenting channel features associated with gas hydrates in the Krishna-Godavari Basin, offshore India. *Marine Geology* 279, 1-11.

Roosta, H., Khosharay, S., Varaminian, F., 2013. Experimental study of methane hydrate formation kinetics with or without additives and modeling based on chemical affinity. *Energy Conversion and Management* 76, 499-505.

Sloan, E.D., Koh, C., 2007. *Clathrate Hydrates of Natural Gases* 3rd ed. CRC Press.

Stern, L.A., Kirby, S.H., Circone, S., Durham, W.B., 2004. Scanning electron microscopy investigations of laboratory-grown gas clathrate hydrates formed from melting ice, and comparison to natural hydrates. *American Mineralogist* 89, 1162-1175.

Tang, X., Lilly, D., Petpisit, K., 2007. Analysis of LWD acoustic data validates its accuracy, 48th Annual Logging Symposium. Society of Petrophysicists and Well-Log Analysts.

Varsamis, G.L., Arian, A., Blanch, J., Market, J., Wisniewski, L., Althoff, G., Barnett, C., 2000. LWD Shear Velocity Logging in Slow Formations Design Decisions and Case Histories, SPWLA 41st Annual Logging Symposium. Society of Petrophysicists and Well-Log Analysts.

Vysniauskas, A., Bishnoi, P.R., 1983. A kinetic study of methane hydrate formation. *Chemical Engineering Science* 38, 1061-1072.

Wang, Z., 2001. Fundamentals of seismic rock physics. *Geophysics* 66, 398-412.

Windmeier, C., Oellrich, L.R., 2013. Theoretical Study of Gas Hydrate Decomposition Kinetics: Model Predictions. *The Journal of Physical Chemistry A* 117, 12184-12195.

Figures:

Figure 1. Mixed hydrate-arrangement cartoons. a) Disconnected fractures modeled with lower HS bounds and b) interconnected fractures modeled with modified upper HS bounds. In (a) and (b) hydrate is attached to mineral grains and both hydrate and water is present in the fractures.

Figure 2. Model inputs. (a) Porosity (b) Saturation. In (a) LWD and Wireline neutron porosity (ϕ) are respectively shown in red and blue. Measured porosity of core samples from the Wireline hole are shown in black dots. LWD porosity, which is lower than Wireline porosity, appears to be closer to the in-situ conditions. The estimated fracture porosity (ϕ_f), assuming 55% background porosity (ϕ_s), for LWD and Wireline is shown in green and black respectively. In (b) saturation from core depressurization is shown with solid black dots. The blue and red lines are input saturations to the model in the Wireline and LWD holes computed as $(S_{hr} * \phi_f + S_{hs} * \phi_s) / \phi$, where S_{hr} and S_{hs} are hydrate saturation in fractures and sediments respectively. The predicted velocities using the porosity and saturation inputs are shown in Figure 3.

Figure 3. Model outputs. (a) Wireline V_p , (b) Wireline V_s and (c) LWD V_p . In (a), (b) and (c) the log data are in black, predicted data with disconnected fractures (lower HS bound) are in red and predicted with interconnected fracture (modified upper SH bound) is in green. For individual logs, the mean is shown in dashed black line and the zone of standard deviation is shaded in transparent yellow.

Figure 4. Hydrate volume fraction (saturation * porosity) in the background (dashed), Wireline fractures (blue) and LWD fractures (red). This figure and 2(b) suggest that although there is minor intra-site variation in hydrate saturation between the Wireline and LWD holes, there is a large change in fracture abundance (ϕ_f roughly doubles from LWD to Wireline hole).

Figure 5. Line scan images. The core from high resistivity zone, 10D-12E, shows a higher connectivity in fractures as compare to the core from lower resistivity zone, 10D-22E. It is possible that hydrate-filled fracture connectivity not only increases elastic velocity but also resistivity. Note the resistivity change at 90 mbsf, which could be related to a change in sediment character.

Tables:

System Components	Density(g/cc)	Bulk Modulus (Gpa)	Shear Modulus(Gpa)
Clay	2.58	21	7
Quartz	2.65	36	45
Hydrates	0.91	7.7	3.2
Water	1.033	2.37	0

Table 1: Parameters used for rock physics modeling

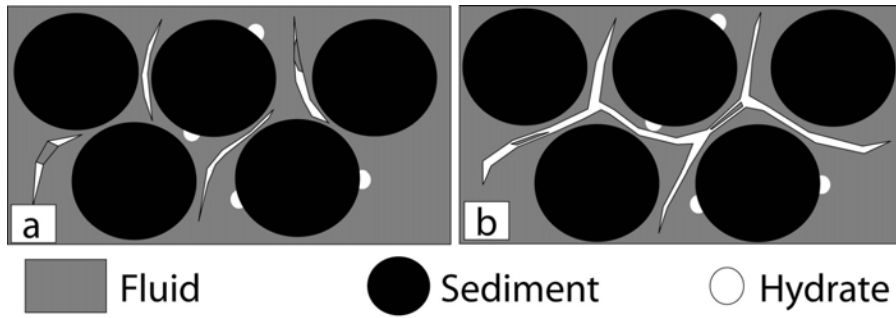


Fig.1

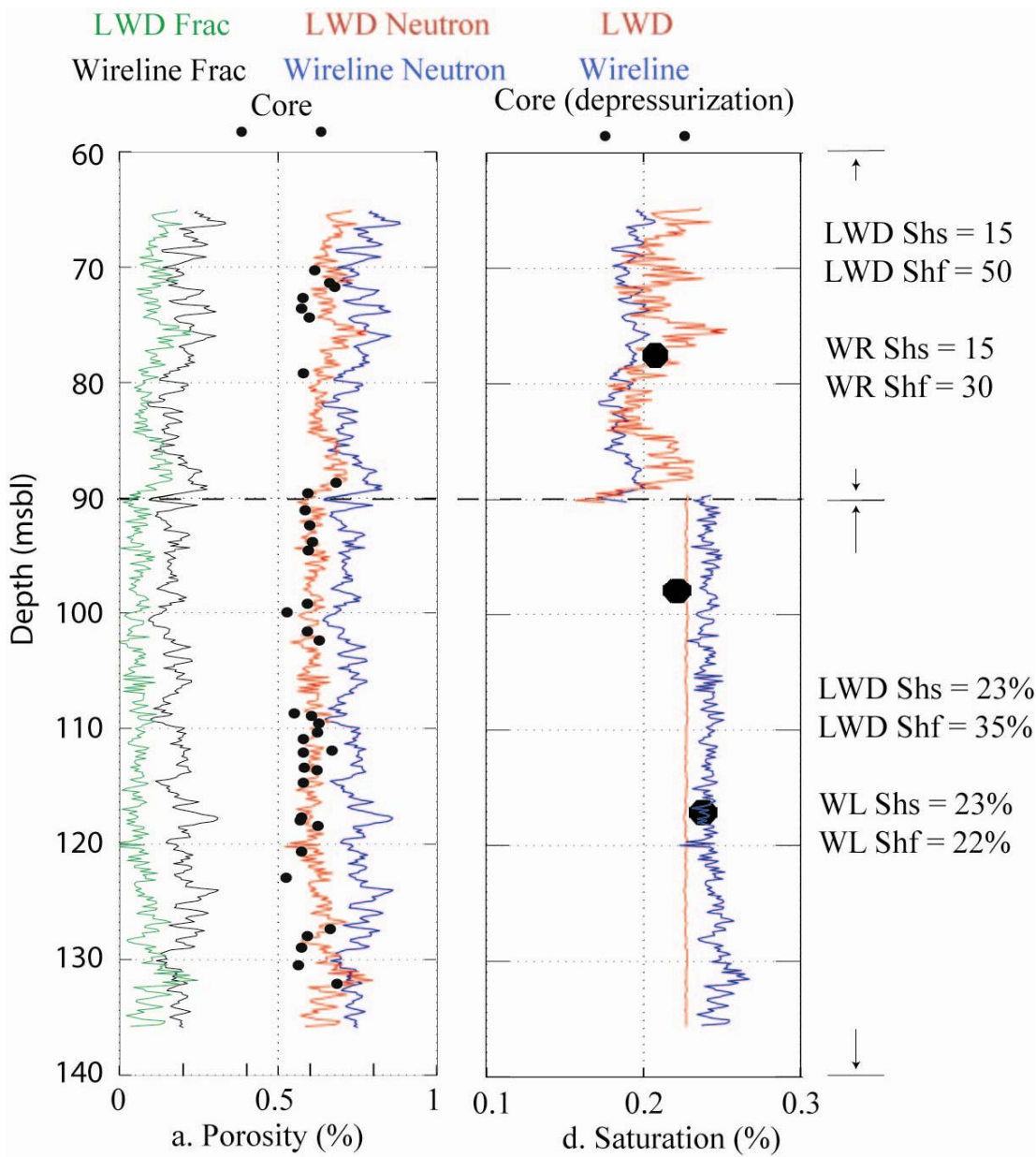


Figure 2

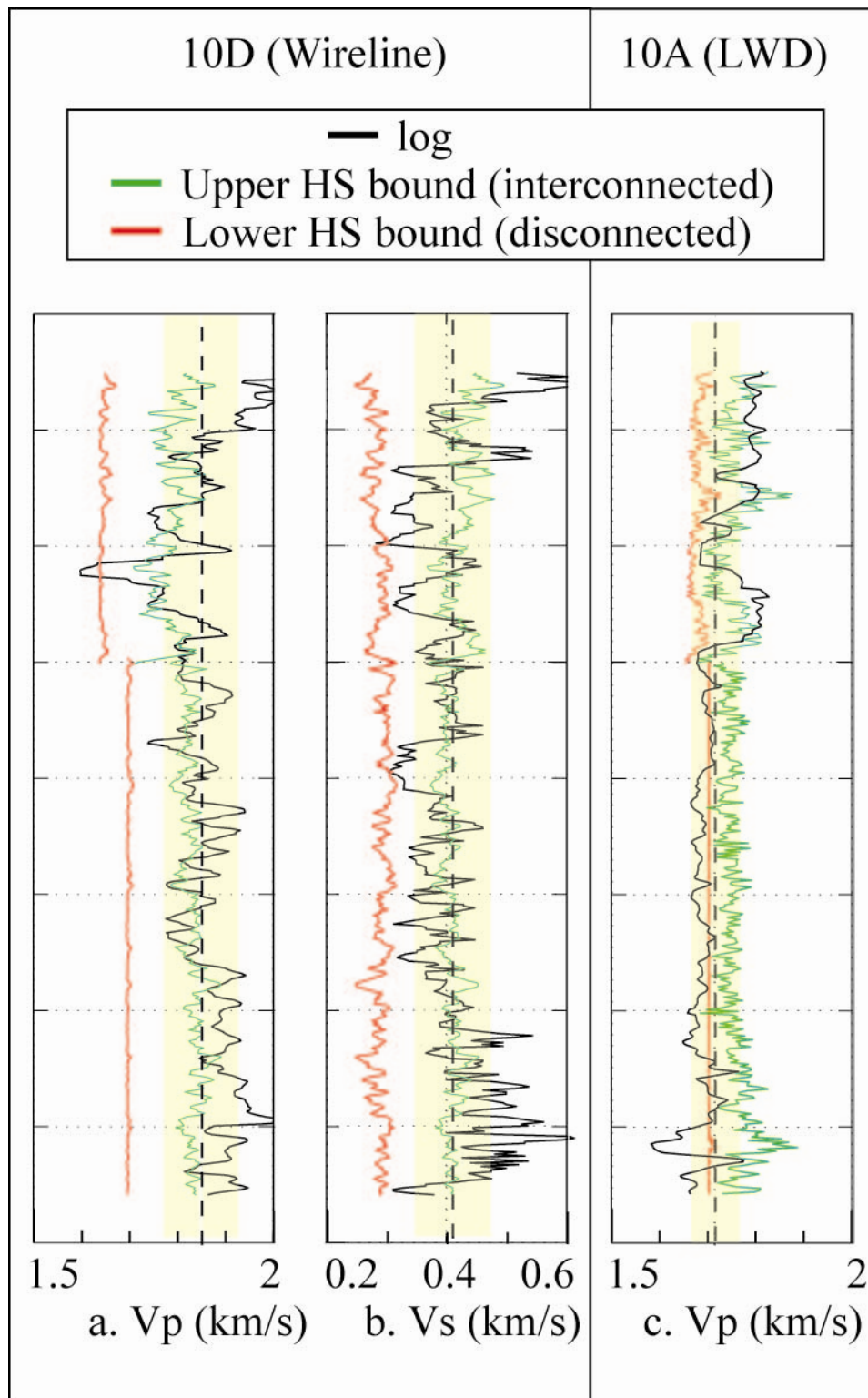


Figure 3.

..... 10A/D $S_{hs} * \phi_s$
 — 10D $S_{hf} * \phi_f$
 — 10A

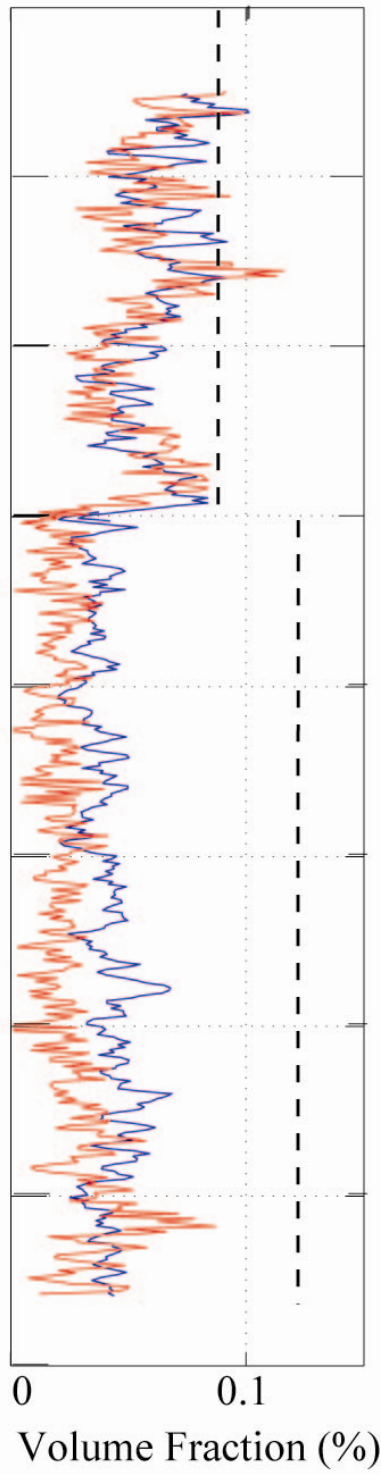


Figure 4.

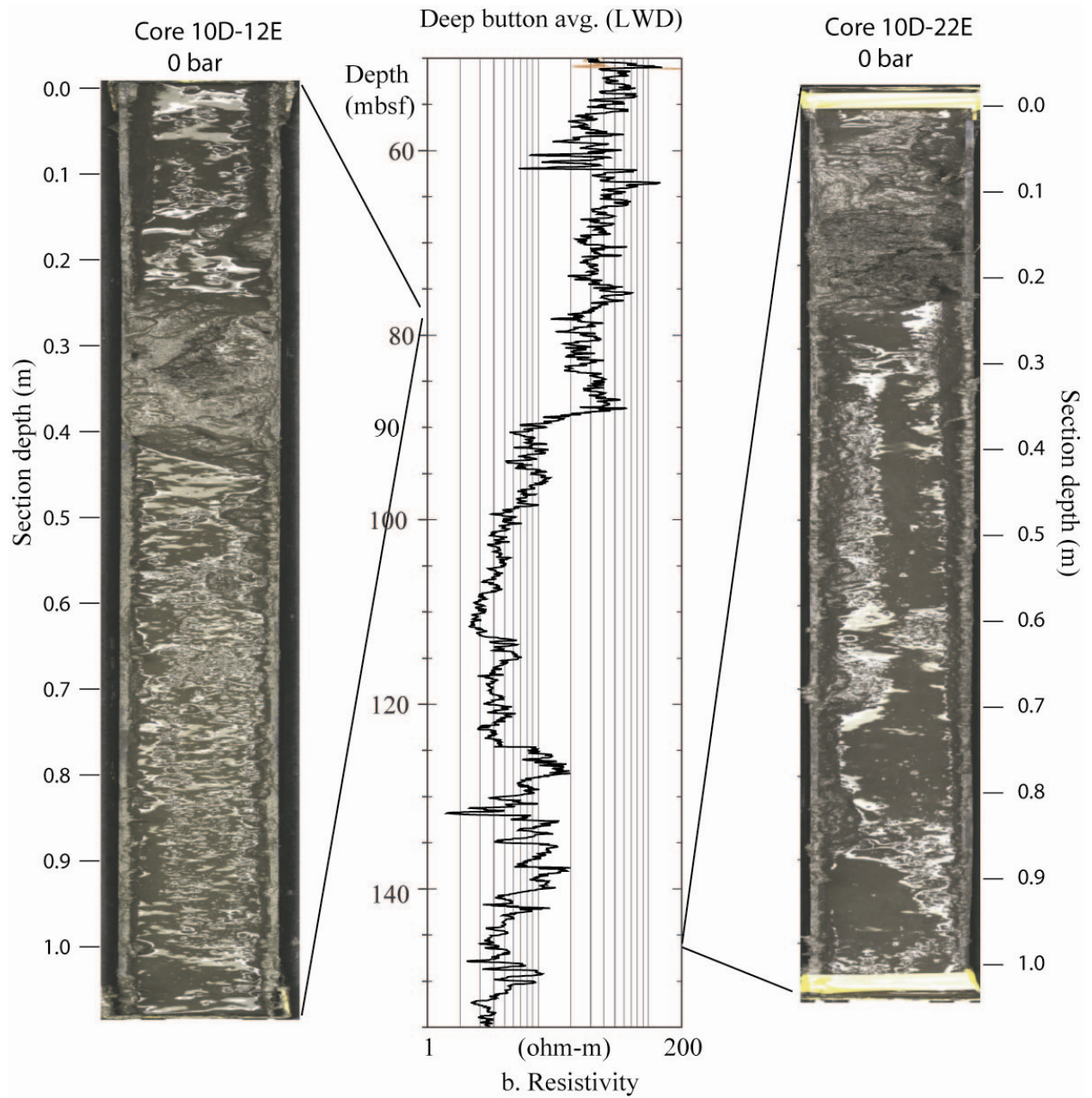


Figure 5.